HOXB1 Founder Mutation in Humans Recapitulates the Phenotype of Hoxb1−/− Mice

Bryn D. Webb,[1,2,29] Sherin Shaaban,[4,8,11,14,15,29] Harald Gaspar,[1,16,28,29] Luis F. Cunha,[1,17] Christian R. Schubert,[10,11,13,18,19] Ke Hao,[1] Caroline D. Robson,[7] Wai-Man Chan,[4,9,20] Caroline Andrews,[4,8,11,20] Sarah MacKinnon,[6] Darren T. Oystreck,[21,22] David G. Hunter,[6,12] Anthony J. Iacovelli,[1] Xiaoqian Ye,[1] Anne Camminady,[16] Elizabeth C. Engle,[4,5,6,8,9,10,11,12,20,23,]* and Ethylin Wang Jabs[1,2,3,24,25,26,27,]*

Members of the highly conserved homeobox (HOX) gene family encode transcription factors that confer cellular and tissue identities along the antero-posterior axis of mice and humans. We have identified a founder homozygous missense mutation in HOXB1 in two families from a conservative German American population. The resulting phenotype includes bilateral facial palsy, hearing loss, and strabismus and correlates extensively with the previously reported Hoxb1−/− mouse phenotype. The missense variant is predicted to result in the substitution of a cysteine for an arginine at amino acid residue 207 (Arg207Cys), which corresponds to the highly conserved Arg5 of the homeodomain. Arg5 interacts with thymine in the minor groove of DNA through hydrogen bonding and electrostatic attraction. Molecular modeling and an in vitro DNA-protein binding assay predict that the mutation would disrupt these interactions, destabilize the HOXB1:PBX1:DNA complex, and alter HOXB1 transcriptional activity.

Congenital facial paralysis (CFP) has been classified among the congenital cranial dysinnervation disorders (CCDDs).[1–3] CFP could be inherited, and autosomal-dominant loci have been mapped for isolated CFP (HCFP1 locus) and for CFP with variable hearing loss (HCFP2 locus).[4–6] CFP can also occur together with complex congenital eye-movement disorders, and in particular as a component of Moebius syndrome (MIM 157900). Moebius syndrome was defined at the Moebius Syndrome Foundation Research Conference in 2007 as congenital, nonprogressive facial weakness with limited abduction of one or both eyes (inability to move the eye fully outward or toward the ear).[7] Additional features can include hearing loss and other cranial nerve dysfunction, as well as motor, orofacial, musculo-skeletal, neurodevelopmental, and social problems.[1,8,9] Moebius syndrome is most frequently sporadic, and with the exception of rare HOXA1 (MIM 142955) or TUBB3 (MIM 602661) mutations that cause atypical Moebius syndromes, its genetics remain undefined.[10,11] Sorting out its genetics has been complicated, in part, by the not-infrequent misdiagnosis of Moebius syndrome in children who have CFP but do not have limited abduction of the eye.

In an effort to identify causative mutations for Moebius syndrome and CFP, we in the Jabs and Engle laboratories enrolled probands diagnosed with these and related disorders and their family members in ongoing genetic studies. The Jabs study was approved by the institutional review boards at The Johns Hopkins University and Mount Sinai School of Medicine, and the Engle study was approved by the institutional review board of Boston Children's Hospital. Written informed consent was obtained from participating family members or from their guardians. All investigations were conducted in accordance with the principles of the Declaration of Helsinki.

[1]Department of Genetics and Genomic Sciences, Mount Sinai School of Medicine, New York, New York 10029, USA; [2]Department of Pediatrics, Mount Sinai School of Medicine, New York, New York 10029, USA; [3]Department of Developmental and Regenerative Biology, Mount Sinai School of Medicine, New York, New York 10029, USA; [4]Department of Neurology, Boston Children's Hospital, 300 Longwood Ave, Boston, MA 02115, USA; [5]Department of Medicine (Genetics), Boston Children's Hospital, 300 Longwood Ave, Boston, MA 02115, USA; [6]Department of Ophthalmology, Boston Children's Hospital, 300 Longwood Ave, Boston, MA 02115, USA; [7]Department of Radiology, Boston Children's Hospital, 300 Longwood Ave, Boston, MA 02115, USA; [8]F.B. Kirby Neurobiology Center, Boston Children's Hospital, 300 Longwood Ave, Boston, MA 02115, USA; [9]Program in Genomics, Boston Children's Hospital, 300 Longwood Ave, Boston, MA 02115, USA; [10]Manton Center for Orphan Disease Research, Boston Children's Hospital, 300 Longwood Ave, Boston, MA 02115, USA; [11]Department of Neurology, Harvard Medical School, Boston, MA 02115, USA; [12]Department of Ophthalmology, Harvard Medical School, Boston, MA 02115, USA; [13]Department of Pediatrics, Harvard Medical School, Boston, MA 02115, USA; [14]Department of Ophthalmology, Mansoura University, Daqahlia 35516, Egypt; [15]Dubai Harvard Foundation for Medical Research, Boston, MA 02115, USA; [16]Institut für Humangenetik, Universitätsklinikum Heidelberg, Heidelberg D-69120, Germany; [17]Human Oncology and Pathogenesis Program, Sloan-Kettering Cancer Center, New York, New York 10065, USA; [18]Research Laboratory of Electronics, Harvard-MIT Division of Health Sciences and Technology, Massachusetts Institute of Technology, Cambridge, MA 02139, USA; [19]Department of Electrical Engineering and Computer Science, Harvard-MIT Division of Health Sciences and Technology, Massachusetts Institute of Technology, Cambridge, MA 02139, USA; [20]Howard Hughes Medical Institute, 4000 Jones Bridge Road, Chevy Chase, MD 20815, USA; [21]Department of Ophthalmology, College of Medicine, King Saud University, Riyadh 11411, Saudi Arabia; [22]Division of Ophthalmology, Faculty of Health Sciences, University of Stellenbosch, Tygerberg 7505, South Africa; [23]The Broad Institute of Harvard and MIT, 301 Binney Street, Cambridge, MA 02142, USA; [24]Department of Pediatrics, School of Medicine, The Johns Hopkins University, Baltimore, MD 21205, USA; [25]Department of Plastic and Reconstructive Surgery, School of Medicine, The Johns Hopkins University, Baltimore, MD 21205, USA; [26]Department of Medicine, School of Medicine, The Johns Hopkins University, Baltimore, MD 21205, USA; [27]Institute of Genetic Medicine, The Johns Hopkins University, Baltimore, MD 21205, USA; [28]Institute of Human Genetics, University Medical Center Freiburg, Freiburg, Germany
[29]These authors contributed equally to this work
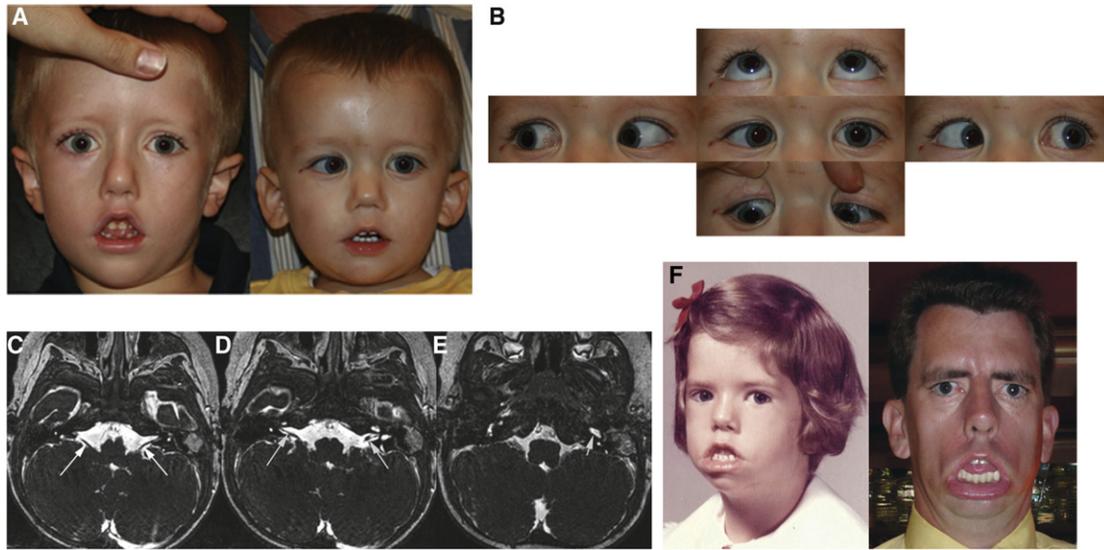*Correspondence: elizabeth.engle@childrens.harvard.edu (E.C.E.), ethylin.jabs@mssm.edu (E.W.J.)

Figure 1. Clinical and Neuroimaging Phenotype of Patients Harboring the Homozygous *HOXB1* c.619C>T mutation

(A) Photographs of affected brothers from family A show a "masked facies" appearance secondary to bilateral facial weakness (patients VI-1 and VI-3 in Figure 2A). Dysmorphic features including midface retrusion, an upturned nasal tip, and low-set and posteriorly rotated ears are noted (Figure S1). Residual postoperative right concomitant esotropia is seen in the younger brother (VI-3), pictured on the right.

(B) Gaze positions of the younger affected brother in family A (VI-3) reveal full ocular motility with right esotropia, thus ruling out Moebius syndrome. Primary gaze (center), right gaze (left), left gaze (right), upgaze (top), and downgaze (bottom).

(C–E) Axial 3D FIESTA (fast imaging employing steady state acquisition) MR imaging of the older brother in family A (VI-1) at 8 months of age. (C) Image is taken through the posterior fossa at the level of the internal auditory meati. The vestibulocochlear nerves (arrows) are demonstrated exiting the pontomedullary junction bilaterally and traversing the cerebellopontine angle cisterns. The facial nerves are not visualized and would ordinarily be expected to travel ventrally and parallel to the VIIIth cranial nerves. (D) Image is a more caudal view demonstrating the right vestibulocochlear nerve (arrow) entering the internal auditory meatus; there is no evidence of a facial nerve in its expected location more ventrally. The vestibulocochlear nerve (arrow) is demonstrated bifurcating into the cochlear and inferior vestibular nerves at a level caudal to the expected location of the VIIth cranial nerve. (E) Image is a more caudal view that reveals subtle bilateral abnormal tapering of the basal turn of the cochlea (short arrow).

(F) Photographs of affected siblings from family B were taken of the sister as a young child and the brother as an adult (patients II-2 and II-4 in Figure 2B). Both have masked facies and bilateral facial weakness, as exhibited in the brother's attempt to smile. The brother has a postoperative right exotropia that is probably secondary to overcorrection. Both siblings also have midface retrusion, an upturned nasal tip, and micrognathia. The brother has low-set ears.

We began by examining two affected brothers who had been born to consanguineous parents of conservative German American background and who had both been diagnosed with Moebius syndrome (patients VI-1 and VI-3 in Figures 1A and 1B and Figure 2A). These siblings were noted to have bilateral facial weakness, sensorineural hearing loss, and esotropia in the first months of life, and they developed feeding difficulties and speech delays requiring oromotor and speech therapies. Both boys underwent surgery to correct esotropia, one at 22 months of age and the other at 4 years, 2 months, and both wear glasses for high hyperopia. Hearing aids were prescribed but not well tolerated. MRI in the older brother (VI-1) at 8 months of age revealed a bilateral absence of the facial nerve and bilateral abnormal tapering of the basal turn of the cochlea (Figures 1C, 1D, and 1E). For both boys, auditory brainstem response (ABR) testing revealed bilateral mild to moderate high-frequency hearing loss with normal absolute latencies of waveforms, and distortion product otoacoustic emissions (DPOAE) were absent in both children, supporting abnormal cochlear function. Stapedius reflexes were intact bilaterally.

At the time of our examination, the boys were 7 years, 3 months and 2 years, 11 months of age. Both brothers have midface retrusion, low-set and posteriorly rotated ears, an upturned nasal tip, and a smooth philtrum. (Figure 1A; see also Figure S1 in the Supplemental Data available with this article online). Neither child showed any facial movement. Taste discrimination, salivation, and lacrimation were intact, as was general sensation over the concha of the ear and skin behind the auricle. Both boys had partially accommodative esotropia with high hyperopia and full eye movements (Figure 1B) and thus did not meet the diagnostic criteria for Moebius syndrome. The parents (IV-3 and V-1 in Figure 2A) and unaffected brother (VI-2 in Figure 2A) were healthy, and neither they nor more distant relatives had strabismus or facial weakness. The father (IV-3) reported a history of speech delay as a child and was noted to have bilateral right > left sensorineural hearing loss; imaging for structural etiologies was not performed. The mother (V-1), unaffected brother (VI-2), and extended family (Figure 2A) reported normal hearing. The mother (V-1) reported no history of fetal loss.
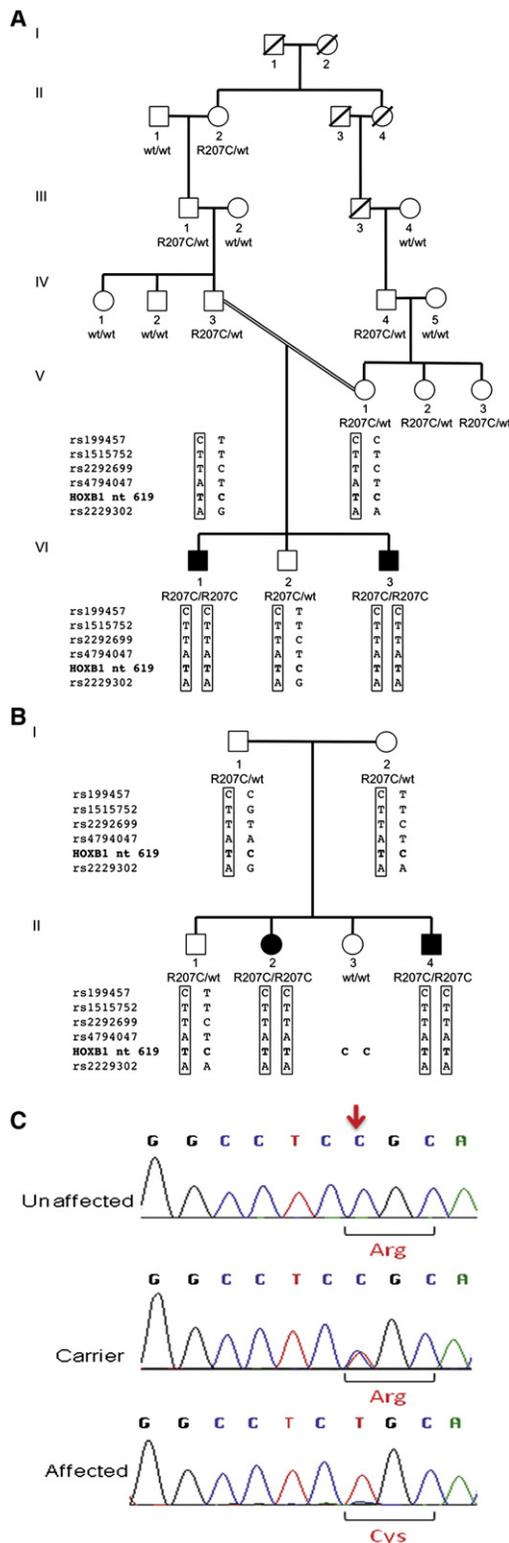
Figure 2. Family Structure, Genotyping, and Haplotype Analysis
(A and B) Schematic representations of pedigree structures, founder haplotype, and mutation status of families A (A) and B (B). Squares denote males, circles denote females, and shaded symbols denote affected individuals. Individuals were genotyped for 20 tagging SNPs on chromosome 17q21: centromere- ***rs199457***, *rs3760377*, *rs2002537*, ***rs1515752***, ***rs2292699***, ***rs4794047***, *rs6503934*, *rs3897986*, *rs1533057*, *rs1509635*, *rs17697950*, *rs6504280*, *rs1553748*, *rs11869101*, *rs925284*, *rs11079824*, *rs10853100*,

To identify the genetic cause of the phenotype in the two affected boys, we conducted linkage and homozygosity mapping of the two affected boys and their parents. A single ~30 Mb region of homozygosity shared by both affected brothers was identified on chromosome 17q21.31–17q25.1, flanked by *rs9900383* and *rs4969059* (Figure S2A). There were no other regions of homozygosity greater than 1 Mb in size, and no pathogenic copy-number variants were identified. We subsequently enrolled 11 additional family members and performed targeted linkage analysis of the extended family. Linkage and haplotype analysis refined the region to 27 Mb (Figure S2B). A maximum two-point LOD score of 2.3 was obtained for all fully informative markers across the critical interval.

Because the 27 Mb region of homozygosity contains more than 400 genes, we proceeded with whole-exome sequencing of DNA from affected individual VI-3 (dbGAP study accession number: phs000478.v1.p1). A total of 19,625 exome variants were identified and filtered, resulting in retention of five missense variants (Table S1). Each variant was confirmed by Sanger sequencing to be homozygous in both affected boys, heterozygous in the unaffected sibling and parents, and to otherwise segregate appropriately within the extended family (Figure 2C; see also Figure S2B). Because hypoplasia of the facial nucleus in *Hoxb1* $^{-/-}$ mice results in congenital facial paralysis, we noted with particular interest the *HOXB1* c.619C>T missense change (MIM 142968, RefSeq accession number NM_002144, RefSeq version number NM_002144.3), predicted to result in the substitution of a polar uncharged cysteine for a highly conserved, positively charged arginine at HOXB1 residue 207 (Arg207Cys; Figures 3A and 3B). Polyphen2,[12] SIFT[13] and PMut[14] predict this amino acid substitution to be damaging, and MUpro predicts with a confidence score of −0.07 that it decreases protein stability.[15] Calculation of the Grantham score, which is 180 for an arginine-to-cysteine alteration, also predicts a radical substitution.[16,17] Moreover, this *HOXB1* c.619C>T nucleotide change is absent from dbSNP132,[18] the 1000 Genomes Project,[19] and the Exome Variant Server (NHLBI Exome Sequencing Project, Seattle, WA).

To determine the frequency of *HOXB1* variants among individuals with similar diagnoses, we sequenced *HOXB1* in 175 additional mutation-negative probands, of whom

rs11079828, *rs8073963*, and ***rs2229302***- telomere. The mutation occurs between *rs10853100* and *rs11079828*. A parsimony approach was used for phasing haplotypes. Representative haplotypes consisting of five SNPs that are informative in these two families are shown (bolded above). The disease-bearing haplotype is boxed, and this haplotype is shared on chromosomes with the *HOXB1* c.619C>T mutation in both families.
(C) Chromatograms of an unaffected individual (top), a mutation carrier (middle), and an affected individual (bottom). There is a homozygous C>T substitution at residue 207 in the affected individual in the position indicated by the red arrow. The wild-type and altered amino acid residues are noted below each sequence.
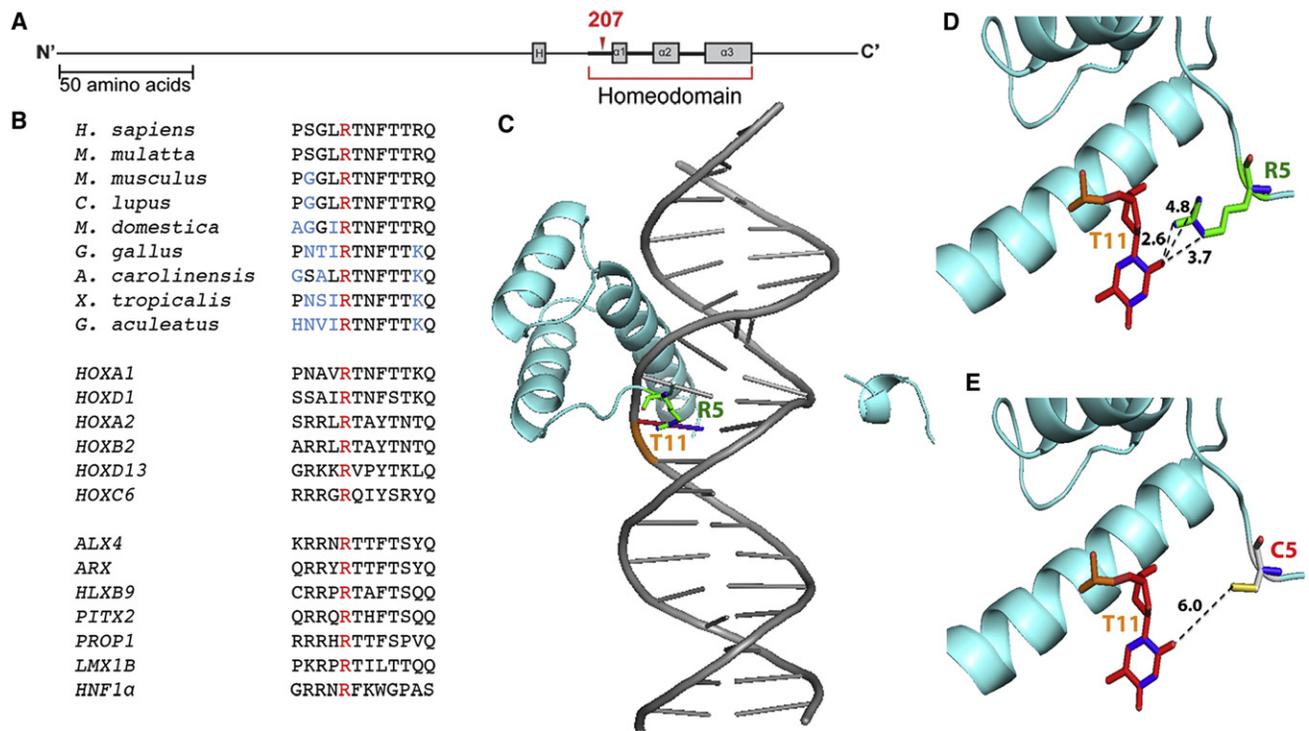
Figure 3. HOXB1 Protein Structure, Conservation, and Molecular Modeling

(A) A two-dimensional schematic representation of HOXB1 highlights the homeodomain (in red brackets), containing 3 α helices and an N-terminal arm. The Arg207Cys amino acid substitution, indicated by the red arrow head, falls in the N-terminal arm of the homeodomain. The H indicates the position of an Antp-type hexapeptide motif.

(B) HOXB1 Arg207 corresponds to the Arg5 residue of the HOXB1 homeodomain. This residue is highly conserved phylogenetically (top) and among other human HOX proteins (middle). Arg5 is also conserved in other homeodomain-containing proteins (bottom), for which mutations altering Arg5 cause human disease.

(C–E) Protein modeling of the Arg207Cys mutation in the HOXB1:PBX1:DNA ternary complex (PDB:1B72). (C and D) Wild-type Arg5 residue (green R5) of the HOXB1 homeodomain interacts with the O2 atoms of the T11 base of the DNA with three hydrogen bonds at 2.6Å, 3.7Å, and 4.8Å. (E) The sulfur atom of mutant Arg5Cys residue (red C5) of the HOXB1 homeodomain would interact with the oxygen atom of T11 base of the DNA via one hydrogen bond at 6.0Å.

102 were diagnosed with Moebius syndrome. The remainder had various combinations of facial weakness, hearing loss, and complex or common strabismus. We identified the identical, homozygous missense variant c.619C>T (p.Arg207Cys) in two affected adult siblings of a second family diagnosed with Moebius syndrome (Patients II-2 and II-4 in Figures 2B and Figure 1F). No other putative mutations were identified among the cohort. The second family is also of conservative German American (Pennsylvania Dutch) background but is not known to be consanguineous. The sister (II-2) had congenital bilateral facial weakness, esophoria at both near and far distances, and mild hearing loss of unknown origin; she did not requiring hearing aids as a child. Her younger brother (II-4) had congenital bilateral facial weakness and sensorineural hearing loss. He wore glasses and had undergone strabismus surgery as a child for "lazy crossed eyes," most consistent with the diagnosis of esotropia. Both siblings had micrognathia, normal intelligence, and no other known anomalies. The mother (I-2 in Figure 2B) had no history of fetal loss.

To further confirm that the c.619C>T variant is not a rare SNP, we sequenced 374 chromosomes from control individuals known to be of German ancestry and 584 additional chromosomes from controls known to be of European descent, and none harbored the c.619C>T variant. Due to the common German heritage in both families, we next examined whether the variant was on a shared haplotype. We chose twenty tagging SNPs on chromosome 17q21 for haplotype analysis over a region of 1.82 Mb, and we determined that the *HOXB1* c.619C>T mutation was on a shared haplotype, centromere-CGCTTATAAGGTGTT ATTGA-telomere (Figures 2A and 2B). Using data obtained from the 1000 Genomes database for these 20 SNPs, we determined that there were 402 different haplotypes among 381 European individuals. The haplotype shared by families A and B was also found in six of the normal European controls, and thus the frequency of this haplotype in the European population is calculated to be 0.787%. Additionally, we were able to distinguish the disease-associated haplotype shared by families A and B from the other possibilities in the European population by using information from only six SNPs (centromere-*rs199457, rs3760377, rs1515752, rs2292699, rs4794047, rs2229302*- telomere); this simplified centromere-CGTTAA-telomere haplotype was also observed six times in the

1000 Genomes data set, or 0.787% in the European population. Because the *HOXB1* c.619C>T mutation occurred in two separate German American families on the same infrequent haplotype background, these results support a founder mutation.

HOXB1 is a member of the highly conserved Homeobox (*HOX*) gene family, which encodes homeodomain-containing transcription factors that confer specificity of spatial-temporal patterning in vertebrates, *Drosophila* and *C. elegans*.[20,21] Humans have 39 *HOX* genes arranged in four paralogous groups—*HOXA, HOXB, HOXC,* and *HOXD*.[22,23] Within each group, genes are expressed in numerical order both temporally and spatially along the antero-posterior axis, where they specify cellular and tissue identities.[24]

The HOXB1 protein is composed of 301 amino acids with the 60 amino acid homeodomain located from amino acid 203 to 262. The homeodomain comprises a flexible N-terminal arm followed by three alpha helices.[25] Arg207, altered by the missense mutation in the two affected families, is located in the N-terminal arm and corresponds to the arginine at position 5 (Arg5) of the homeodomain (Figures 3A, 3C, and 3D). Previous studies have demonstrated that the transcriptional specificity of HOX proteins in vivo is determined, in part, by this Arg5, which forms a hydrogen bond with the thymine (T11) in the minor groove of DNA (Figure 3C and 3D).[24,26] Hox transcriptional specificity is also determined by the interaction of Hox proteins with cofactors and collaborator proteins such as the transcriptional coactivator Pbx1, an atypical homeodomain protein; these interactions increase the stability and specificity of the DNA-binding properties of Hox proteins.[26–30] Residue Arg5 maintains its contact with the minor groove when Hox-DNA binding is monomeric, as well as when HOXB1 is part of a cooperative HOXB1:PBX1:DNA complex.[31,32] Moreover, it was previously reported that mutating Arg5 of the homeodomain to alanine in HOXA1 in vitro resulted in a dramatic decrease in the stability of the HOXA1:PBX1A complex.[32] Given that Arg5 is highly conserved among all HOX proteins (Figure 3B), this destabilization model may expand to other HOX protein-PBX interactions, including those involving HOXB1. The importance of the Arg5 residue in humans is further highlighted by the number of disorders resulting from mutations altering Arg5 in other homeodomain-containing proteins, including those encoded by *ALX4* (MIM 605420), *ARX* (MIM 300382), *HLXB9* (MIM 142994), *PITX2* (MIM 601542), *PROP1* (MIM 601538), *LMX1B* (MIM 602575), and *HNF1α* (MIM 142410) (Figure 3B).[33] Among these, pituitary hormone deficiency (MIM 262600) and maturity onset diabetes of the young, type 3 (MODY3) (MIM 600496) are caused specifically by arginine-to-cysteine substitutions in *PROP1* and *HNF1α*, respectively.[34,35]

We took advantage of the publically available crystal structure of the HOXB1:PBX1:DNA ternary complex (PBX1 MIM 176310; Protein Data Bank ID 1B72) to assess the effects of the Arg207Cys substitution in greater molecular detail by using PyMOL (PyMOL Molecular Graphics System, version 1.3, Schrödinger, LLC).[31] In the wild-type (WT) protein, at physiological pH, the interaction between Arg207 and the T11 base in the minor groove of DNA is probably stabilized through both hydrogen bonding and electrostatic attraction. The guanidino group of the Arg207 side chain is ideally positioned to act as both hydrogen bond donor through its side-chain amino group hydrogen atoms and as hydrogen bond acceptor through the lone pair electrons on its side-chain nitrogen atoms, all of which are within 4 Å of the O2 oxygen atom in the T11 base (Figure 3D). In addition, because at pH 7.4 the guanidino group of Arg207 is resonance stabilized and positively charged, it can further participate in electrostatically favorable interactions with the equally resonance-stabilized and negatively charged oxygen atoms in the T11 base in the minor groove of DNA.

In the altered HOXB1 (Figure 3E), it is likely that both hydrogen bonding and electrostatic attractive forces are diminished. The Arg207Cys alteration lengthens the distance between the O2 oxygen atom of the T11 base and the protein residue approximately one and half to two times the distance of the WT protein, effectively outside the energetically favorable length of a hydrogen bond of typically <4.0 Å. In addition, the Arg→Cys substitution is likely to result in electrostatically repulsive forces through the introduction of a negatively charged sulfur atom onto the protein residue: the pKa of the Cys side chain is expected to be ~8.0, and so at physiological pH a fraction of the Cys residues will be negatively charged, i.e., not protonated, and thus repulsive to the negative charge on the resonance-stabilized oxygen atoms in the T11 base.

We also modeled the energetic consequences of the Arg207Cys substitution on DNA binding on the basis of the available crystal structure by using the FoldX algorithm.[36] The protein-DNA binding energy was calculated to be 1.5 kcal/mol higher for the mutant than for the WT protein, which corresponds to a seven-fold-weaker binding constant at room temperature ($\Delta G = -RT \ln [K_{eq}]$). Although consistent with our structural analysis of the pathogenic effects of the Arg207Cys substitution as described above, these energetic consequences would need to be verified experimentally via adequate biophysical analytical methods.

Lastly, we examined the transcriptional ability of the altered HOXB1 Arg207Cys protein in vitro by performing a DNA-protein binding assay. Upstream of *HOXB1* is a key *cis*-regulatory element, which includes three repetitive PBX/HOX binding sites and a SOX/OCT binding site. This element, which is phylogenetically conserved through a variety of species, acts as an enhancer for the expression of HOXB1 and is termed the b1-ARE (auto-regulatory element).[37] DiRocco and colleagues previously showed that both HOXB1 and PBX1 are needed to

A
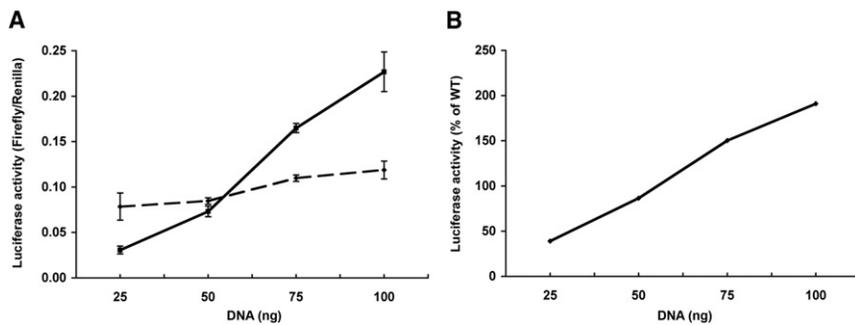

B

cooperatively bind the murine b1-ARE to increase HOXB1 expression.[38] Thus, we performed site-directed mutagenesis to introduce the c.619C>T mutation in the expression vector pSG-HOXB1 and evaluated the effect of the HOXB1 Arg207Cys substitution on transactivation of the b1-ARE by using a luciferase assay (Figure 4). Interestingly, at low DNA concentrations the HOXB1 Arg207Cys substitution had decreased transactivation of the b1-ARE when compared to wild-type, whereas at high DNA concentrations it led to increased transactivation. These findings are similar to the findings of transactivation studies performed by Yamada and colleagues,[34] who compared the HNF1α Arg203Cys substitution, which also corresponds to an Arg5Cys substitution in the homeodomain, to the wild-type in its transactivation of the promoter of *GLUT2* (MIM 138160). Again, at low DNA concentrations, the Arg203Cys protein had decreased luciferase activity, but at high concentrations it had increased activity in comparison to wild-type activity. These findings suggest that the HOXB1 Arg207Cys protein is functionally different from the wild-type.

The phenotype of the individuals harboring the c.619C>T mutation recapitulates the phenotype of the *Hoxb1*$^{-/-}$ mice, further supporting loss of *HOXB1* function. During normal mouse development, *Hoxb1* plays a prominent role in the formation of rhombomere 4 (r4) and its derivatives.[39–42] *Hoxb1* and *Hoxa1* are expressed at early stages in the spinal cord and hindbrain; their anterior boundary is at the r3/r4 interface. Following neuronal differentiation, *Hoxb1* expression is maintained at high levels in r4 and in neural crest cells migrating away from this rhombomere.[43–45] In *Hoxb1*$^{-/-}$ mice, r4 early patterning is initiated normally but is then altered, possibly to an r2 identity.[43,46] The majority of *Hoxb1*$^{-/-}$ mice survive and have facial weakness and degeneration of their facial muscles. There is marked reduction and sometimes complete absence of the facial motor nucleus,[44,46,47] the motor component of the facial nerve is reduced in size, and there is variable thinning, stunting,

or absence of nerve branches between and among animals.[44] This pathology results both from the cell-autonomous role of Hoxb1 in the specification of the r4 facial branchiomotor (FBM) neurons[45,47] and from its non-cell-autonomous role in a subset of *Hoxb1*-positive r4-derived neural crest cells that differentiate into Schwann cells that myelinate the facial nerve and are critical for its maintenance.[46–48] Similar to the *Hoxb1*$^{-/-}$ mice, the affected members of families A and B have bilateral facial paralysis, and the facial nerve could not be seen in the one affected individual imaged by MRI. Moreover, the motor branches are variably affected; although most of the facial muscles are paralyzed, the response of the stapedial muscle is intact.

The sensory component of the facial nerve appears to be normal in *Hoxb1*$^{-/-}$ mutants, whereas the viscero-motor parasympathetic component of the facial nerve, which innervates the salivary glands, was reported to be abnormal in only one of many *Hoxb1*$^{-/-}$ mice examined.[44,46] Similarly, functions of the sensory and parasympathetic components of the facial nerve were tested and were normal in the affected brothers of family A.

The second neuronal population that arises in r4 is the contralateral vestibuloacoustic (CVA) neurons, whose axons project from the pontine superior olivary complex in the olivocochlear bundle (OCB) to innervate hair cells of the organ of Corti. A trophic interaction between the OCB and outer hair cells is thought to be required for development of normal hearing; disruption of the OCB in neonatal cats alters the sensitivity, frequency, selectivity, and spontaneous discharge rates of the auditory nerve fibers and results in sensorineural hearing loss.[49] The predominant effect of the mature olivocochlear reflex is to both enhance the hair cell response to transient noise stimuli and to simultaneously suppress the response to steady background noise.[50] It also serves to protect the ear from permanent acoustic injury from loud noises.[51,52] Although hearing has not been documented in the *Hoxb1*$^{-/-}$ mice, the CVA neurons are not appropriately

specified and fail both to migrate and to send axons to their targets.[43,44,46] Thus, errors in the development of CVA neurons and the OCB innervation of hair cells in the affected family members, coupled with risk of hair cell damage from loud noises, might account for these individuals' sensorineural hearing loss. In addition, neuro-imaging of one affected individual revealed bilateral abnormal tapering of the basal turn of the cochlea, and thus the affected individuals could also be at risk for hearing loss secondary to additional inner-ear malformations. Finally, additional studies are needed if we are to determine whether the heterozygous *HOXB1* mutation is associated with sensorineural hearing loss, given its presence in one of eleven heterozygous mutation carriers (Figures 2A and 2B; see also Figure S2B).

Although all four individuals homozygous for the mutation are affected with CFP, none of these individuals have limited abduction of either eye, and thus they do not meet diagnostic criteria for Moebius syndrome. Normal abduction is consistent with the normal abducens nerve as reported in $Hoxb1^{-/-}$ mice.[45] Remarkably, however, all four affected individuals do have some degree of esodeviation; three have esotropia and one has esophoria, and esodeviation has not been reported in $Hoxb1^{-/-}$ mice. If the strabismus results from the homozygous *HOXB1* mutation, it would suggest that HOXB1 plays a direct or indirect role in the control of binocular alignment. The consanguinity of family A and the apparent relatedness of families A and B, however, raises the possibility that they could share a genetic etiology for strabismus unrelated to *HOXB1*.

In summary, we have identified a *HOXB1* mutation that causes autosomal-recessive congenital facial palsy with sensorineural hearing loss, dysmorphic features, and probably strabismus. Our functional studies demonstrate that the Arg207Cys homeodomain mutation alters binding between the HOXB1:PBX1 protein complex and DNA. It will be necessary to identify additional individuals harboring mutations in *HOXB1* to better define the phenotypic spectrum of this new syndrome, as well as to re-examine the $Hoxb1^{-/-}$ mice in light of these human findings.

Supplemental Data

Supplemental Data include two figures and one table and can be found with this article online at http://www.cell.com/AJHG/.

Acknowledgments

Web Resources

The URLs for data presented herein are as follows:

dbGAP study accession of whole-exome data, http://www.ncbi.nlm.nih.gov/projects/gap/cgi-bin/study.cgi?study_id=phs000478.v1.p1

dbSNP, http://www.ncbi.nlm.nih.gov/projects/SNP/

Exome Variant Server, NHLBI Exome Sequencing Project (ESP), Seattle, WA, http://evs.gs.washington.edu/EVS/

NCBI Reference Sequence (RefSeq), http://www.ncbi.nlm.nih.gov/RefSeq/

Online Mendelian Inheritance in Man (OMIM), http://www.omim.org/

PolyPhen-2, http://genetics.bwh.harvard.edu/pph2/

Primer3, http://frodo.wi.mit.edu/

RCSB Protein Data Bank, http://www.rcsb.org/pdb/

University of California Santa Cruz Genome Bioinformatics, http://genome.ucsc.edu/

1000 Genomes, http://www.1000genomes.org/

Accession Numbers

The dbGAP Study Accession number for the whole exome sequence reported in this paper is phs000478.v1.p1.

References

1. Oystreck, D.T., Engle, E.C., and Bosley, T.M. (2011). Recent progress in understanding congenital cranial dysinnervation disorders. J. Neuroophthalmol. 31, 69–77.

2. Gutowski, N.J., Bosley, T.M., and Engle, E.C. (2003). 110th ENMC International Workshop: The congenital cranial dysinnervation disorders (CCDDs). Naarden, The Netherlands, 25-27 October, 2002. Neuromuscul. Disord. 13, 573–578.

3. Traboulsi, E.I. (2007). Congenital cranial dysinnervation disorders and more. J. AAPOS 11, 215–217.

4. Kremer, H., Kuyt, L.P., van den Helm, B., van Reen, M., Leunissen, J.A., Hamel, B.C., Jansen, C., Mariman, E.C., Frants, R.R., and Padberg, G.W. (1996). Localization of a gene for Möbius syndrome to chromosome 3q by linkage analysis in a Dutch family. Hum. Mol. Genet. 5, 1367–1371.

5. Verzijl, H.T., van den Helm, B., Veldman, B., Hamel, B.C., Kuyt, L.P., Padberg, G.W., and Kremer, H. (1999). A second gene for autosomal dominant Möbius syndrome is localized

to chromosome 10q, in a Dutch family. Am. J. Hum. Genet. *65*, 752–756.

6. Alrashdi, I.S., Rich, P., and Patton, M.A. (2010). A family with hereditary congenital facial paresis and a brief review of the literature. Clin. Dysmorphol. *19*, 198–201.

7. Miller, G. (2007). Neurological disorders. The mystery of the missing smile. Science *316*, 826–827.

8. Verzijl, H.T., van der Zwaag, B., Cruysberg, J.R., and Padberg, G.W. (2003). Möbius syndrome redefined: A syndrome of rhombencephalic maldevelopment. Neurology *61*, 327–333.

9. Bogart, K.R., and Matsumoto, D. (2010). Living with Moebius syndrome: Adjustment, social competence, and satisfaction with life. Cleft Palate Craniofac. J. *47*, 134–142.

10. Tischfield, M.A., Bosley, T.M., Salih, M.A., Alorainy, I.A., Sener, E.C., Nester, M.J., Oystreck, D.T., Chan, W.M., Andrews, C., Erickson, R.P., and Engle, E.C. (2005). Homozygous HOXA1 mutations disrupt human brainstem, inner ear, cardiovascular and cognitive development. Nat. Genet. *37*, 1035–1037.

11. Tischfield, M.A., Baris, H.N., Wu, C., Rudolph, G., Van Maldergem, L., He, W., Chan, W.M., Andrews, C., Demer, J.L., Robertson, R.L., et al. (2010). Human TUBB3 mutations perturb microtubule dynamics, kinesin interactions, and axon guidance. Cell *140*, 74–87.

12. Adzhubei, I.A., Schmidt, S., Peshkin, L., Ramensky, V.E., Gerasimova, A., Bork, P., Kondrashov, A.S., and Sunyaev, S.R. (2010). A method and server for predicting damaging missense mutations. Nat. Methods *7*, 248–249.

13. Kumar, P., Henikoff, S., and Ng, P.C. (2009). Predicting the effects of coding non-synonymous variants on protein function using the SIFT algorithm. Nat. Protoc. *4*, 1073–1081.

14. Ferrer-Costa, C., Gelpí, J.L., Zamakola, L., Parraga, I., de la Cruz, X., and Orozco, M. (2005). PMUT: A web-based tool for the annotation of pathological mutations on proteins. Bioinformatics *21*, 3176–3178.

15. Cheng, J., Randall, A., and Baldi, P. (2006). Prediction of protein stability changes for single-site mutations using support vector machines. Proteins *62*, 1125–1132.

16. Grantham, R. (1974). Amino acid difference formula to help explain protein evolution. Science *185*, 862–864.

17. Li, W.H., Wu, C.I., and Luo, C.C. (1984). Nonrandomness of point mutation as reflected in nucleotide substitutions in pseudogenes and its evolutionary implications. J. Mol. Evol. *21*, 58–71.

18. Sherry, S.T., Ward, M.H., Kholodov, M., Baker, J., Phan, L., Smigielski, E.M., and Sirotkin, K. (2001). dbSNP: the NCBI database of genetic variation. Nucleic Acids Res. *29*, 308–311.

19. 1000 Genomes Project Consortium. (2010). A map of human genome variation from population-scale sequencing. Nature *467*, 1061–1073.

20. Krumlauf, R. (1994). Hox genes in vertebrate development. Cell *78*, 191–201.

21. McGinnis, W., and Krumlauf, R. (1992). Homeobox genes and axial patterning. Cell *68*, 283–302.

22. Scott, M.P. (1992). Vertebrate homeobox gene nomenclature. Cell *71*, 551–553.

23. Faiella, A., Zortea, M., Barbaria, E., Albani, F., Capra, V., Cama, A., and Boncinelli, E. (1998). A genetic polymorphism in the human HOXB1 homeobox gene implying a 9bp tandem repeat in the amino-terminal coding region. Mutations in brief no. 200. Online. Hum. Mutat. *12*, 363.

24. Mann, R.S., Lelli, K.M., and Joshi, R. (2009). Hox specificity unique roles for cofactors and collaborators. Curr. Top. Dev. Biol. *88*, 63–101.

25. Gehring, W.J., Affolter, M., and Bürglin, T. (1994). Homeodomain proteins. Annu. Rev. Biochem. *63*, 487–526.

26. Mann, R.S. (1995). The specificity of homeotic gene function. Bioessays *17*, 855–863.

27. Chang, C.P., Shen, W.F., Rozenfeld, S., Lawrence, H.J., Largman, C., and Cleary, M.L. (1995). Pbx proteins display hexapeptide-dependent cooperative DNA binding with a subset of Hox proteins. Genes Dev. *9*, 663–674.

28. Knoepfler, P.S., and Kamps, M.P. (1995). The pentapeptide motif of Hox proteins is required for cooperative DNA binding with Pbx1, physically contacts Pbx1, and enhances DNA binding by Pbx1. Mol. Cell. Biol. *15*, 5811–5819.

29. Moens, C.B., and Selleri, L. (2006). Hox cofactors in vertebrate development. Dev. Biol. *291*, 193–206.

30. Mann, R.S., and Chan, S.K. (1996). Extra specificity from extradenticle: The partnership between HOX and PBX/EXD homeodomain proteins. Trends Genet. *12*, 258–262.

31. Piper, D.E., Batchelor, A.H., Chang, C.P., Cleary, M.L., and Wolberger, C. (1999). Structure of a HoxB1-Pbx1 heterodimer bound to DNA: role of the hexapeptide and a fourth homeodomain helix in complex formation. Cell *96*, 587–597.

32. Phelan, M.L., and Featherstone, M.S. (1997). Distinct HOX N-terminal arm residues are responsible for specificity of DNA recognition by HOX monomers and HOX.PBX heterodimers. J. Biol. Chem. *272*, 8635–8643.

33. Chi, Y.I. (2005). Homeodomain revisited: a lesson from disease-causing mutations. Hum. Genet. *116*, 433–444.

34. Yamada, S., Tomura, H., Nishigori, H., Sho, K., Mabe, H., Iwatani, N., Takumi, T., Kito, Y., Moriya, N., Muroya, K., et al. (1999). Identification of mutations in the hepatocyte nuclear factor-1alpha gene in Japanese subjects with early-onset NIDDM and functional analysis of the mutant proteins. Diabetes *48*, 645–648.

35. Vallette-Kasic, S., Pellegrini-Bouiller, I., Sampieri, F., Gunz, G., Diaz, A., Radovick, S., Enjalbert, A., and Brue, T. (2001). Combined pituitary hormone deficiency due to the F135C human Pit-1 (pituitary-specific factor 1) gene mutation: Functional and structural correlates. Mol. Endocrinol. *15*, 411–420.

36. Guerois, R., Nielsen, J.E., and Serrano, L. (2002). Predicting changes in the stability of proteins and protein complexes: A study of more than 1000 mutations. J. Mol. Biol. *320*, 369–387.

37. Ishioka, A., Jindo, T., Kawanabe, T., Hatta, K., Parvin, M.S., Nikaido, M., Kuroyanagi, Y., Takeda, H., and Yamasu, K. (2011). Retinoic acid-dependent establishment of positional information in the hindbrain was conserved during vertebrate evolution. Dev. Biol. *350*, 154–168.

38. Di Rocco, G., Mavilio, F., and Zappavigna, V. (1997). Functional dissection of a transcriptionally active, target-specific Hox-Pbx complex. EMBO J. *16*, 3644–3654.

39. Gavalas, A., Davenne, M., Lumsden, A., Chambon, P., and Rijli, F.M. (1997). Role of Hoxa-2 in axon pathfinding and rostral hindbrain patterning. Development *124*, 3693–3702.

40. Gavalas, A., Ruhrberg, C., Livet, J., Henderson, C.E., and Krumlauf, R. (2003). Neuronal defects in the hindbrain of Hoxa1, Hoxb1 and Hoxb2 mutants reflect regulatory interactions among these Hox genes. Development *130*, 5663–5679.

41. Gavalas, A., Studer, M., Lumsden, A., Rijli, F.M., Krumlauf, R., and Chambon, P. (1998). Hoxa1 and Hoxb1 synergize in patterning the hindbrain, cranial nerves and second pharyngeal arch. Development *125*, 1123–1136.

42. Rossel, M., and Capecchi, M.R. (1999). Mice mutant for both Hoxa1 and Hoxb1 show extensive remodeling of the hindbrain and defects in craniofacial development. Development *126*, 5027–5040.

43. Briscoe, J., and Wilkinson, D.G. (2004). Establishing neuronal circuitry: Hox genes make the connection. Genes Dev. *18*, 1643–1648.

44. Goddard, J.M., Rossel, M., Manley, N.R., and Capecchi, M.R. (1996). Mice with targeted disruption of Hoxb-1 fail to form the motor nucleus of the VIIth nerve. Development *122*, 3217–3228.

45. Guthrie, S. (2007). Patterning and axon guidance of cranial motor neurons. Nat. Rev. Neurosci. *8*, 859–871.

46. Studer, M., Lumsden, A., Ariza-McNaughton, L., Bradley, A., and Krumlauf, R. (1996). Altered segmental identity and abnormal migration of motor neurons in mice lacking Hoxb-1. Nature *384*, 630–634.

47. Arenkiel, B.R., Tvrdik, P., Gaufo, G.O., and Capecchi, M.R. (2004). Hoxb1 functions in both motoneurons and in tissues of the periphery to establish and maintain the proper neuronal circuitry. Genes Dev. *18*, 1539–1552.

48. Arenkiel, B.R., Gaufo, G.O., and Capecchi, M.R. (2003). Hoxb1 neural crest preferentially form glia of the PNS. Dev. Dyn. *227*, 379–386.

49. Walsh, E.J., McGee, J., McFadden, S.L., and Liberman, M.C. (1998). Long-term effects of sectioning the olivocochlear bundle in neonatal cats. J. Neurosci. *18*, 3859–3869.

50. Kawase, T., Delgutte, B., and Liberman, M.C. (1993). Antimasking effects of the olivocochlear reflex. II. Enhancement of auditory-nerve response to masked tones. J. Neurophysiol. *70*, 2533–2549.

51. Kujawa, S.G., and Liberman, M.C. (1997). Conditioning-related protection from acoustic injury: Effects of chronic deefferentation and sham surgery. J. Neurophysiol. *78*, 3095–3106.

52. Maison, S.F., and Liberman, M.C. (2000). Predicting vulnerability to acoustic injury with a noninvasive assay of olivocochlear reflex strength. J. Neurosci. *20*, 4701–4707.